Uniform Channel Decomposition for MIMO Communications

Yi Jiang, *Student Member, IEEE*, Jian Li, *Fellow, IEEE*, and William W. Hager

***Abstract*—Assuming the availability of the channel state information at the transmitter (CSIT) and receiver (CSIR), we consider the joint optimal transceiver design for multi-input multi-output (MIMO) communication systems. Using the geometric mean decomposition (GMD), we propose a transceiver design that can decompose, in a *strictly* capacity lossless manner, a MIMO channel into multiple subchannels with *identical* capacities. This uniform channel decomposition (UCD) scheme has two implementation forms. One is the combination of a linear precoder and a minimum mean-squared-error VBLAST (MMSE-VBLAST) detector, which is referred to as UCD-VBLAST, and the other includes a dirty paper (DP) precoder and a linear equalizer followed by a DP decoder, which we refer to as UCD-DP. The UCD scheme can provide much convenience for the modulation/demodulation and coding/decoding procedures due to obviating the need for bit allocation. We also show that UCD can achieve the maximal diversity gain. The simulation results show that the UCD scheme exhibits excellent performance, even without the use of any error correcting codes.**

***Index Terms*—Channel capacity, DBLAST, dirty paper precoder, diversity gain, geometric mean decomposition, joint transceiver design, MIMO, minimum mean-squared-error, VBLAST, water filling.**

I. Introduction

COMMUNICATIONS over multiple-input multiple-output (MIMO) channels have been the subject of intense research over the past several years because MIMO channels can support much greater data rate and higher reliability than their single-input single-output (SISO) counterpart [1], [2]. The majority of the researches focus on the scenarios where only the channel state information at receiver (CSIR) is available. Nevertheless, if the communication environment is slowly time varying, such as communications via indoor wireless local area networks (WLANs) or data transmission via the bonded digital subscriber lines (DSLs), the channel state information at the transmitter (CSIT) is also possible via feedback or the reciprocal principle when time division duplex (TDD) is used. Based on this assumption, the joint optimal transceiver design has recently attracted considerable attention (see [3] and the references therein). Almost all the researchers have concentrated on the linear transceiver designs. To maximize the channel throughput, the channel must be diagonalized via the singular value decomposition (SVD). Due to the usually large condition number of the channel matrix, the SVD-based channel decomposition usually results in subchannels with vastly different signal-to-noise ratios (SNRs), which can add much complexity to the subsequent modulation/demodulation and coding/decoding procedures. For example, to achieve the channel capacity, bit allocation (see, e.g., [4]) is required to match each subchannel capacity, which not only makes modulation rather complicated but also causes capacity loss due to the finite constellation granularity. On the other hand, if the same constellation is used for each subchannel, like the schemes adopted by the European standard HIPERLAN/2 and the IEEE 802.11 standards for wireless local area networks (WLANs), then more power should be allocated to the poorer subchannels, which can lead to considerable performance loss [5]. There is apparently a tradeoff between the channel throughput and the bit-error-rate (BER) performance if one attempts to avoid bit allocation. We show the contrary as detailed below.

An efficient nonlinear transceiver design based on the geometric mean decomposition (GMD) algorithm is proposed in [5]. By combining the GMD matrix decomposition algorithm [6] with either the zero-forcing VBLAST (ZF-VBLAST) detector [7] or the zero-forcing dirty paper precoder (ZFDP), the GMD scheme[1] decomposes a MIMO channel into multiple *identical* parallel subchannels. The GMD scheme has proven to be asymptotically optimal for high SNR in both the channel throughput and the BER performance aspects. Hence, the GMD scheme does not make tradeoffs between the capacity and the BER performance. Instead, it attempts to achieve the best of both worlds simultaneously. However, the GMD scheme may suffer from considerable capacity loss at low SNR due to the inherent "zero-forcing" operations, which are capacity lossy, especially at low SNR.

In this paper, we propose a uniform channel decomposition (UCD) scheme, which is also based on the GMD matrix decomposition algorithm to decompose a MIMO channel into multiple *identical* subchannels. The UCD scheme has two implementation forms. One is the combination of a linear precoder and a minimum mean-squared-error VBLAST (MMSE-VBLAST) detector, which is referred to as UCD-VBLAST, and the other includes a dirty paper (DP) precoder and a linear equalizer followed by a DP decoder, which we refer to as UCD-DP. Just

Manuscript received July 7, 2004; revised December 12, 2004. This work was supported in part by the National Science Foundation under Grant CCR-0104887. The associate editor coordinating the review of this manuscript and approving it for publication was Dr. Petar M. Djuric.

Y. Jiang was with the Department of Electrical and Computer Engineering, University of Florida, Gainesville, FL 32611-6130 USA. He is now with the Uiversity of Colorado, Boulder, CO 80309 USA (e-mail: yjiang@dsp.colorado.edu).

J. Li with the Department of Electrical and Computer Engineering, University of Florida, Gainesville, FL 32611-6130 USA (e-mail: li@dsp.ufl.edu).

W. W. Hager is with the Department of Mathematics, University of Florida, Gainesville, FL 32611-8105 USA (e-mail: hager@math.ufl.edu).

Digital Object Identifier 10.1109/TSP.2005.857052

[1]In the sequel, we refer to the GMD scheme or GMD as the MIMO transceiver design based on the GMD matrix decomposition algorithm.

1053-587X/$20.00 © 2005 IEEE

like the GMD scheme, UCD can bring much convenience to the subsequent modulation/demodulation and coding/decoding procedures by obviating the need of bit allocation. Two remarkable merits of UCD, which are not shared by the GMD scheme, are that first, UCD is *strictly* capacity lossless at any SNR, and second, UCD has the maximal diversity gain. Moreover, the UCD scheme can decompose a MIMO channel into an arbitrarily large number of independent subchannels, which is an enabling technology to achieve high data rate transmission using small symbol constellations. The UCD scheme suggests a new way of channel decomposition, which can decompose a MIMO channel into multiple subchannels with desired channel capacities [8]. This is much more flexible than the conventional SVD-based approaches.

The rest of this paper is organized as follows. Section II introduces the channel model. Section III briefly reviews of the VBLAST scheme, the dirty paper theorem, and the GMD scheme. A closed-form expression of the MMSE-VBLAST detector, which is proven to be very useful for the UCD design, is also introduced. Two versions of the UCD scheme, i.e., UCD-VBLAST and UCD-DP, are proposed in Section IV. We also compare the diversity gains of UCD and the GMD scheme therein. Section V presents several numerical examples to demonstrate the advantages of the UCD scheme over GMD and the open-loop VBLAST scheme. Finally, Section VI gives the conclusions of this paper.

II. Channel Model

We consider a communication system with M_t transmitting and M_r receiving antennas in a frequency flat fading channel. The sampled baseband signal is given by

$$\mathbf{y} = \mathbf{H}\mathbf{F}\mathbf{x} + \mathbf{z} \tag{1}$$

where $\mathbf{x} \in \mathbb{C}^{L\times 1}$ is the information symbols precoded by the linear precoder $\mathbf{F} \in \mathbb{C}^{M_t\times L}$, $\mathbf{y} \in \mathbb{C}^{M_r\times 1}$ is the received signal, and $\mathbf{H} \in \mathbb{C}^{M_r\times M_t}$ is the channel matrix with rank K and with its (i,j)th element denoting the fading coefficient between the jth transmitting and ith receiving antennas. We assume $E[\mathbf{x}\mathbf{x}^*] = \sigma_x^2\mathbf{I}_L$, where $E[\cdot]$ is the expected value, $\mathbf{I}_L$ denotes the identity matrix with dimension L, and $\mathbf{z} \sim N(0, \sigma_z^2\mathbf{I}_{M_r})$ is the circularly symmetric complex Gaussian noise. We define the SNR as

$$\rho = \frac{E[\mathbf{x}^*\mathbf{F}^*\mathbf{F}\mathbf{x}]}{\sigma_z^2} = \frac{\sigma_x^2}{\sigma_z^2}\mathrm{Tr}\{\mathbf{F}^*\mathbf{F}\} \triangleq \frac{1}{\alpha}\mathrm{Tr}\{\mathbf{F}^*\mathbf{F}\} \tag{2}$$

where $(\cdot)^\circ$ is the conjugate transpose, and $\mathrm{Tr}\{\cdot\}$ stands for the trace of a matrix. Throughout this paper, we assume that $\mathbf{H}$ is known at both the transmitter and receiver. We note that the more general frequency-selective channel can be represented by a spatial-temporal channel with a larger dimensionality. Hence, (1) is rather general.

Suppose $\mathbf{x}$ is a Gaussian random vector. The capacity of the MIMO channel (1) is

$$C = \log_2 \frac{\left|\sigma_z^2\mathbf{I} + \sigma_x^2\mathbf{H}\mathbf{F}\mathbf{F}^*\mathbf{H}^*\right|}{|\sigma_z^2\mathbf{I}|} \tag{3}$$

where $|\cdot|$ denotes the determinant of a matrix. If both CSIT and CSIR are available, we can maximize the channel capacity with respect to $\mathbf{F}$, given the input power constraint $\sigma_x^2\mathrm{Tr}\{\mathbf{F}\mathbf{F}^*\} = \rho\sigma_z^2$. That is

$$C_{IT} = \max_{\sigma_x^2\mathrm{Tr}\{\mathbf{F}\mathbf{F}^*\}=\rho\sigma_z^2} \log_2 |\mathbf{I} + \alpha^{-1}\mathbf{H}\mathbf{F}\mathbf{F}^*\mathbf{H}^*| \tag{4}$$

where α is as defined in (2), and the subscript of C_{IT} stands for "informed transmitter."

Denote the SVD of $\mathbf{H}$ as $\mathbf{H} = \mathbf{U}\mathbf{\Lambda}\mathbf{V}^*$, where $\mathbf{\Lambda}$ is a $K \times K$ diagonal matrix whose diagonal elements $\{\lambda_{H,k}\}_{k=1}^K$ are the nonzero singular values of $\mathbf{H}$. The solution to $\mathbf{F}$ in (4) is [9]

$$\mathbf{F} = \mathbf{V}\mathbf{\Phi}^{\frac{1}{2}}. \tag{5}$$

Here $\mathbf{\Phi}$ is diagonal whose kth $(1 \le k \le K)$ diagonal element ϕ_k determines the power loaded to the kth subchannel and is found via "water filling" to be

$$\phi_k(\mu) = \left(\mu - \frac{\alpha}{\lambda_{H,k}^2}\right)^+ \tag{6}$$

where μ is chosen such that $\sigma_x^2\sum_{k=1}^K \phi_k(\mu) = \rho\sigma_z^2$ and $(a)^+ = \max\{0, a\}$. Then, the solution to (4) is

$$C_{IT} = \sum_{k=1}^K \log_2\left(1 + \frac{\phi_k}{\alpha}\lambda_{H,k}^2\right) \text{bits/s/Hz}. \tag{7}$$

Note that since some of ϕ_k's can be zeros. In this case, we can only transmit $L < K$ data streams.

Indeed, the linear precoder $\mathbf{F}$ of (5) combined with a linear MMSE equalizer represents a linear transceiver design that is optimal in the information-theoretic aspect. However, due to the usually very different $\{\lambda_{H,k}\}_{k=1}^K$, the linear transceiver leads to multiple subchannels with very different SNRs. Hence, this seemingly simple linear transceiver can bring much difficulty to the subsequent modulation/demodulation and coding/decoding procedures.

III. Preliminaries

In this section, we give a brief review of the concepts of the VBLAST detector and DP precoder, which are the components of UCD-VBLAST and UCD-DP, respectively. We also give a brief introduction to the GMD scheme since the UCD scheme shares the same underlying idea as the GMD scheme. Finally, a closed-form expression of the MMSE-VBLAST algorithm, on which the UCD scheme relies, is introduced.

A. ZF-VBLAST

It is well-known that the ZF-VBLAST scheme can be represented by the QR decomposition $\mathbf{H} = \mathbf{Q}\mathbf{R}$, where $\mathbf{R}$ is an $M_t \times M_t$ upper triangular matrix, and $\mathbf{Q}$ is an $M_r \times M_t$ matrix with its orthonormal columns being the ZF nulling vectors. Let us rewrite (1) as

$$\mathbf{y} = \mathbf{Q}\mathbf{R}\mathbf{x} + \mathbf{z}. \tag{8}$$

Multiplying $\mathbf{Q}^*$ to both sides of (8), which is virtually the *nulling step*, yields

$$\tilde{\mathbf{y}} = \mathbf{R}\mathbf{x} + \tilde{\mathbf{z}} \tag{9}$$

or

$$\begin{bmatrix} \tilde{y}_1 \\ \tilde{y}_2 \\ \vdots \\ \tilde{y}_{M_t} \end{bmatrix} = \begin{bmatrix} r_{11} & r_{12} & \cdots & r_{1M_t} \\ 0 & r_{22} & \cdots & r_{2M_t} \\ \vdots & \ddots & \ddots & \vdots \\ 0 & \ldots & 0 & r_{M_tM_t} \end{bmatrix} \begin{bmatrix} x_1 \\ x_2 \\ \vdots \\ x_{M_t} \end{bmatrix} + \begin{bmatrix} \tilde{z}_1 \\ \tilde{z}_2 \\ \vdots \\ \tilde{z}_{M_t} \end{bmatrix}. \tag{10}$$

The sequential signal detection, which involves the *successive interference cancellation*, is as follows:

```
for i = M_t : -1 : 1
  x̂_i = C[ỹ_i - Σ_{j=i+1}^{M_t} r_ij x̂_j / r_ii]
end
```

Ignoring the error-propagation effect, we see that the MIMO channel is decomposed into M_t parallel scalar subchannels

$$\tilde{y}_i = r_{ii}x_i + \tilde{z}_i, \quad i = 1, 2, \ldots, M_t. \tag{11}$$

B. DP Precoder

As a dual form of the known interference cancellation at the receiver, the DP precoder can be used at the transmitter [10], [11] to suppress known interferences at transmitter.

Consider a scalar Gaussian channel

$$y = x + s + z \tag{12}$$

where s, z are independent Gaussian noise with s known to the receiver. Clearly, the channel of (12) is exactly the same as the additive white Gaussian noise (AWGN) channel

$$y = x + z \tag{13}$$

since the receiver can cancel out the known-interference s prior to signal detection. This is what the VBLAST detector does at the em cancellation step.

Now, reconsider the channel of (12), where the interference s is *unknown* to the receiver but known to the transmitter. The *dirty paper theorem* [12] predicts the existence of an amazing precoder that can cancel out the interference completely without consuming additional input power. That is, we can still obtain an equivalent AWGN channel $y = x + z$.

As the practical implementation of the dirty paper precoder, the Tomlinson–Harashima precoder [13] can be used to achieve known-interference cancellation at the transmitter with only a small amount of power amplification.

C. GMD

The GMD algorithm is based on the following lemma. [We abuse the notation slightly for the sake of notational simplicity. The matrices $\mathbf{Q}, \mathbf{R}$ given in Lemma III.1 are not related to those given in (8).]

Lemma III.1: Any rank K matrix $\mathbf{H} \in \mathbb{C}^{M_r \times M_t}$ with singular values $\lambda_{H,1} \geq \lambda_{H,2} \geq \ldots \geq \lambda_{H,K} > 0$ can be decomposed into

$$\mathbf{H} = \mathbf{Q}\mathbf{R}\mathbf{P}^* \tag{14}$$

where $\mathbf{R} \in \mathbb{R}^{K \times K}$ is an upper triangular matrix with equal diagonal elements

$$r_{ii} = \bar{\lambda}_H \triangleq \left(\prod_{n=1}^{K} \lambda_{H,n} \right)^{\frac{1}{K}}, \quad 1 \leq i \leq K \tag{15}$$

and $\mathbf{Q} \in \mathbb{C}^{M_r \times K}$ and $\mathbf{P} \in \mathbb{C}^{M_t \times K}$ have orthonormal columns.

Proof: See [5]. ■

We present, in [6], a computationally efficient and numerically stable algorithm to calculate (14). To facilitate our discussions and to make this paper self-contained, we include the GMD algorithm in Appendix A.

Assuming CSIT, we can make the precoder $\mathbf{F} = \mathbf{P}$. Hence, the received signal of (1) is

$$\mathbf{y} = \mathbf{Q}\mathbf{R}\mathbf{x} + \mathbf{z}. \tag{16}$$

Multiplying $\mathbf{Q}^*$ to both sides of (16) yields

$$\tilde{\mathbf{y}} = \mathbf{R}\mathbf{x} + \tilde{\mathbf{z}}. \tag{17}$$

Hence, using either the sequential detected signal cancellation or the DP precoding, we can cancel the interference due to the off-diagonal elements of $\mathbf{R}$ and obtain K *identical* scalar subchannels

$$\tilde{y}_i = \bar{\lambda}_H x_i + \tilde{z}_i, \quad i = 1, 2, \ldots, K. \tag{18}$$

The GMD scheme can bring much convenience to the subsequent modulation/demodulation and coding/decoding procedures, and it has superior performance over the linear transceiver designs, as demonstrated in [5]. However, it may suffer from considerable capacity loss at low SNR. Indeed, the major motivation of this paper is to eliminate the capacity loss while preserving all the desirable properties of the GMD scheme. The proposed solution is the UCD scheme, which also relies on the GMD matrix decomposition algorithm. It also relies on the closed-form representation of the MMSE-VBLAST detector.

D. Closed-Form Representation of MMSE-VBLAST

For MMSE-VBLAST, the nulling vector for the ith layer is

$$\mathbf{w}_i = \left(\sum_{j=1}^{i} \mathbf{h}_j \mathbf{h}_j^* + \alpha \mathbf{I} \right)^{-1} \mathbf{h}_i, \quad i = 1, \ldots, M_t. \tag{19}$$

The MMSE-VBLAST algorithm can be represented in a concise matrix form that was given in [14] (also see the more detailed version [15]).

Consider the augmented matrix

$$\mathbf{H}_a = \begin{bmatrix} \mathbf{H} \\ \sqrt{\alpha}\mathbf{I}_{M_t} \end{bmatrix}_{(M_r+M_t)\times M_t}. \tag{20}$$

Applying the QR decomposition to $\mathbf{H}_a$ yields

$$\mathbf{H}_a = \mathbf{Q}_{H_a}\mathbf{R}_{H_a} \triangleq \begin{bmatrix}\mathbf{Q}^u_{H_a}\\ \mathbf{Q}^l_{H_a}\end{bmatrix}\mathbf{R}_{H_a} \tag{21}$$

where $\mathbf{R}_{H_a} \in \mathbb{C}^{M_t\times M_t}$ is an upper triangular matrix with positive diagonal elements, and $\mathbf{Q}^u_{H_a} \in \mathbb{C}^{M_r\times M_t}$. Note that $\mathbf{H} = \mathbf{Q}^u_{H_a}\mathbf{R}_{H_a}$ is *not* the QR decomposition of $\mathbf{H}$ since $\mathbf{Q}^u_{H_a}$ is not unitary. However, we can readily obtain the nulling vectors using $\mathbf{Q}^u_{H_a}$ and $\mathbf{R}_{H_a}$, as shown in the following lemma [15].

Lemma III.2: Let $\{\mathbf{q}_{H_a,i}\}_{i=1}^{M_t}$ denote the columns of $Q^u_{H_a}$ and $\{r_{H_a,ii}\}_{i=1}^{M_t}$ the diagonal elements of $\mathbf{R}_{H_a}$, where $\mathbf{Q}^u_{H_a}$ and $\mathbf{R}_{H_a}$ are given in (21). The nulling vectors of (19) satisfy

$$\mathbf{w}_i = r^{-1}_{H_a,ii}\mathbf{q}_{H_a,i}, \quad i = 1,2,\ldots,M_t. \tag{22}$$

Then, the output signal-to-interfere-and-noise ratio (SINR) of the ith layer (i.e., the signal corresponding to $\mathbf{h}_i$) using $\mathbf{w}_i$ is

$$\rho_i = \frac{|\mathbf{h}_i^*\mathbf{w}_i|^2\sigma_x^2}{\mathbf{w}_i^*\left(\sum_{j=1}^{i-1}\sigma_x^2\mathbf{h}_j\mathbf{h}_j^* + \sigma_z^2\mathbf{I}\right)\mathbf{w}_i}. \tag{23}$$

Inserting (19) into (23), we can simplify (23) via some straightforward calculations to be (see, e.g., [16])

$$\rho_i = \mathbf{h}_i^*\mathbf{C}_i^{-1}\mathbf{h}_i, \quad i = 1,\ldots,M_t \tag{24}$$

where $\mathbf{C}_i = \sum_{j=1}^{i=1}\mathbf{h}_j\mathbf{h}_j^* + \alpha\mathbf{I}$.

The SINRs given in (24) are related to $\mathbf{R}_{H_a}$, as shown in the following lemma.

Lemma III.3: The diagonal of $\mathbf{R}_{H_a}$ given in (21) and $\{\rho_i\}_{i=1}^{M_t}$ given in (24) satisfy

$$\alpha(1+\rho_i) = r^2_{H_a,ii}, \quad i = 1,2,\ldots,M_t. \tag{25}$$

Proof: See Appendix B. ■

An immediate corollary follows.

Corollary III.4: The MMSE-VBLAST detector is information lossless. That is

$$\sum_{i=1}^{M_t}\log(1+\rho_i) = \log|\mathbf{H}^*\mathbf{H}\alpha^{-1} + \mathbf{I}| \tag{26}$$

where the right-hand side of (26) is equal to (4) with $\mathbf{F} = \mathbf{I}_{M_t}$.

The proof is omitted. We note that Corollary III.4 coincides with the findings in [16]. In spite of the capacity lossless property, MMSE-VBLAST suffers from poor diversity gain.

IV. Uniform Channel Decomposition

In the following, we introduce the UCD-VBLAST scheme, which consists of a linear precoder and the MMSE-VBLAST detector. Then, we present the UCD-DP scheme as the dual form of UCD-VBLAST. We also compare the UCD and GMD schemes in terms of diversity gain. Our further remarks are provided at the end of this section.

A. UCD-VBLAST

If we modify the precoder $\mathbf{F}$ given in (5) to be

$$\mathbf{F} = \mathbf{V}\mathbf{\Phi}^{\frac{1}{2}}\mathbf{\Omega}^* \tag{27}$$

where $\mathbf{\Omega} \in \mathbb{C}^{L\times K}$ with $L \geq K$ (to avoid capacity loss, we should not choose $L < K$ in general) and $\mathbf{\Omega}^*\mathbf{\Omega} = \mathbf{I}$, then we see, by inserting (27) into (4), that the $\mathbf{F}$ given in (27) is also a precoder maximizing the channel throughput. However, introducing $\mathbf{\Omega}$ brings much greater flexibility than the precoder of (5). In the following, we concentrate on how to design $\mathbf{\Omega}$.

Given the precoder of (27), the virtual channel is

$$\mathbf{G} \triangleq \mathbf{HF} = \mathbf{U}\mathbf{\Lambda}\mathbf{\Phi}^{\frac{1}{2}}\mathbf{\Omega}^* \triangleq \mathbf{U}\mathbf{\Sigma}\mathbf{\Omega}^* \tag{28}$$

where $\mathbf{\Sigma} = \mathbf{\Lambda}\mathbf{\Phi}^{1/2}$ is a diagonal matrix with diagonal elements for $\{\sigma_i\}_{i=1}^K$. Let $\mathbf{G}_a$ denote the augmented matrix

$$\mathbf{G}_a = \begin{bmatrix}\mathbf{U}\mathbf{\Sigma}\mathbf{\Omega}^*\\ \sqrt{\alpha}\mathbf{I}_L\end{bmatrix}. \tag{29}$$

The UCD scheme is based on the following lemma.

Lemma IV.1: For any matrix of the form given in (29), we can find a semi-unitary matrix $\mathbf{\Omega} \in \mathbb{C}^{L\times K}$ such that the QR decomposition of $\mathbf{G}_a$ yields an upper triangular matrix with equal diagonal elements.

Proof: Rewrite (29) as

$$\mathbf{G}_a = \begin{bmatrix}\mathbf{U}\left[\mathbf{\Sigma}\vdots\mathbf{0}_{K\times(L-K)}\right]\mathbf{\Omega}_0^*\\ \sqrt{\alpha}\mathbf{I}_L\end{bmatrix} \tag{30}$$

where $\mathbf{\Omega}_0 \in \mathbb{C}^{L\times L}$ is a unitary matrix whose first K columns form $\mathbf{\Omega}$. We further rewrite (30) as

$$\mathbf{G}_a = \begin{bmatrix}\mathbf{I}_{M_r} & \mathbf{0}\\ \mathbf{0} & \mathbf{\Omega}_0\end{bmatrix}\begin{bmatrix}\mathbf{U}\left[\mathbf{\Sigma}\vdots\mathbf{0}_{K\times(L-K)}\right]\\ \sqrt{\alpha}\mathbf{I}_L\end{bmatrix}\mathbf{\Omega}_0^*. \tag{31}$$

From Lemma III.1, we can have the following GMD:

$$\mathbf{J} \triangleq \begin{bmatrix}\mathbf{U}\left[\mathbf{\Sigma}\vdots\mathbf{0}_{K\times(L-K)}\right]\\ \sqrt{\alpha}\mathbf{I}_L\end{bmatrix} = \mathbf{Q}_J\mathbf{R}_J\mathbf{P}_J^* \tag{32}$$

where $\mathbf{R}_J \in \mathbb{R}^{L\times L}$ is an upper triangular matrix with equal diagonal elements, $\mathbf{Q}_J \in \mathbb{C}^{(M_r+L)\times L}$ is semi-unitary, and $\mathbf{P}_J \in \mathbb{C}^{L\times L}$ is unitary. Inserting (32) into (31) yields

$$\mathbf{G}_a = \begin{bmatrix}\mathbf{I}_{M_r} & \mathbf{0}\\ \mathbf{0} & \mathbf{\Omega}_0\end{bmatrix}\mathbf{Q}_J\mathbf{R}_J\mathbf{P}_J^*\mathbf{\Omega}_0^*. \tag{33}$$

Let $\mathbf{\Omega}_0 = \mathbf{P}_J^*$ and

$$\mathbf{Q}_{G_a} = \begin{bmatrix}\mathbf{I}_{M_r} & \mathbf{0}\\ \mathbf{0} & \mathbf{\Omega}_0^*\end{bmatrix}\mathbf{Q}_J. \tag{34}$$

Then, (33) can be rewritten to be $\mathbf{G}_a = \mathbf{Q}_{G_a}\mathbf{R}_J$, which is the QR decomposition of $\mathbf{G}_a$. The semi-unitary matrix $\mathbf{\Omega}$ associated with $\mathbf{G}_a$ consists of the first K columns of $\mathbf{\Omega}_0$ (or $\mathbf{P}_J^*$). ■

From Lemmas IV.1 and III.3, we conclude that we can always combine a linear precoder and the MMSE-VBLAST detector to uniformly decompose a MIMO channel into $L \geq K$ subchannels with the same output SINRs. According to Corollary III.4, we can further conclude that the channel decomposition is strictly capacity lossless. We refer to the scheme demonstrated in Lemma IV.1 as UCD-VBLAST.

The proof of Lemma IV.1 is insightful. Indeed, given the SVD of $\mathbf{H}$ and the "water filling" level $\mathbf{\Phi}^{1/2}$, we only need to calculate the GMD given in (32). Then, we immediately obtain the linear precoder $\mathbf{F} = \mathbf{V}\mathbf{\Phi}^{1/2}\mathbf{\Omega}^*$, where $\mathbf{\Omega}$ consists of the first K columns of $\mathbf{P}_J^*$. Let $\mathbf{Q}^u_{G_a}$ denote the first M_r rows of $\mathbf{Q}_{G_a}$ or,

equivalently, the first M_r rows of $\mathbf{Q}_J$ [cf. (34)]. According to Lemma III.2, the nulling vectors are calculated as

$$\mathbf{w}_i = r_{J,ii}^{-1}\mathbf{q}_{G_a,i}, \quad i = 1, 2, \ldots, L \tag{35}$$

where $r_{J,ii}$ is the ith diagonal element of $\mathbf{R}_J$, and $\mathbf{q}_{G_a,i}$ is the ith column of $\mathbf{Q}_{G_a}^u$.

Some observations can help reduce the computational complexity. For any matrix $\mathbf{B} \in \mathbb{C}^{M\times N}$ with SVD $\mathbf{B} = \mathbf{U}_B\mathbf{\Lambda}_B\mathbf{V}_B^*$ and the augmented matrix with SVD

$$\mathbf{A} = \begin{bmatrix} \mathbf{B} \\ \sqrt{\alpha}\mathbf{I} \end{bmatrix} = \mathbf{U}_A\mathbf{\Lambda}_A\mathbf{V}_A^* \tag{36}$$

the diagonal elements of $\mathbf{\Lambda}_A$ and $\mathbf{\Lambda}_B$, i.e., $\gamma_{A,i}$ and $\gamma_{B,i}$, satisfy

$$\lambda_{A,i} = \sqrt{\lambda_{B,i}^2 + \alpha}, \quad i = 1, \ldots, N. \tag{37}$$

Moreover

$$\mathbf{U}_A = \begin{pmatrix} \mathbf{U}_B\mathbf{\Lambda}_B\mathbf{\Lambda}_A^{-1} \\ \sqrt{\alpha}\mathbf{V}_B^*\mathbf{\Lambda}_A^{-1} \end{pmatrix} \quad \text{and} \quad \mathbf{V}_A = \mathbf{V}_B. \tag{38}$$

Hence, the SVD of $\mathbf{J}$ defined in (32) is

$$\mathbf{J} = \begin{bmatrix} \mathbf{U}\begin{bmatrix} \mathbf{\Sigma} \vdots \mathbf{0}_{K\times(L-K)} \end{bmatrix}\tilde{\mathbf{\Sigma}}^{-1} \\ \sqrt{\alpha}\tilde{\mathbf{\Sigma}}^{-1} \end{bmatrix}\tilde{\mathbf{\Sigma}}\mathbf{I}_L \tag{39}$$

where $\tilde{\mathbf{\Sigma}}$ is an $L\times L$ diagonal matrix with the diagonal elements

$$\tilde{\sigma}_i = \sqrt{\sigma_i^2 + \alpha}, \quad 1 \le i \le K \tag{40a}$$

and

$$\tilde{\sigma}_i = \sqrt{\alpha}, \quad K+1 \le i \le L. \tag{40b}$$

Applying the GMD matrix decomposition algorithm given in Appendix A to $\tilde{\mathbf{\Sigma}}$ yields

$$\tilde{\mathbf{\Sigma}} = (\mathbf{Q}_1\mathbf{Q}_2\ldots\mathbf{Q}_{L-1})\mathbf{R}_J\left(\mathbf{P}_{L-1}^T\mathbf{P}_{L-2}^T\ldots\mathbf{P}_1^T\right). \tag{41}$$

Hence

$$\begin{bmatrix} \mathbf{U}\begin{bmatrix} \mathbf{\Sigma} \vdots \mathbf{0}_{K\times(L-K)} \end{bmatrix} \\ \sqrt{\alpha}\mathbf{I}_L \end{bmatrix} = \begin{bmatrix} \mathbf{U}\begin{bmatrix} \mathbf{\Sigma} \vdots \mathbf{0}_{K\times(L-K)} \end{bmatrix}\tilde{\mathbf{\Sigma}}^{-1} \\ \sqrt{\alpha}\tilde{\mathbf{\Sigma}}^{-1} \end{bmatrix} \times(\mathbf{Q}_1\mathbf{Q}_2\ldots\mathbf{Q}_{L-1})\mathbf{R}_J\left(\mathbf{P}_{L-1}^T\mathbf{P}_{L-2}^T\ldots\mathbf{P}_1^T\right). \tag{42}$$

Then, the linear precoder has the form

$$\mathbf{F} = \mathbf{V}\begin{bmatrix} \mathbf{\Phi}^{\frac{1}{2}} \vdots \mathbf{0}_{K\times(L-K)} \end{bmatrix}\mathbf{P}_1\mathbf{P}_2\ldots\mathbf{P}_{L-1}. \tag{43}$$

The nulling vectors are calculated according to (35) with $r_{J,ii} = (\prod_{i=1}^L \tilde{\sigma}_i)^{1/L}$, and

$$\mathbf{Q}_{G_a}^u = \mathbf{U}\begin{bmatrix} \mathbf{\Sigma} \vdots \mathbf{0}_{K\times(L-K)} \end{bmatrix}\tilde{\mathbf{\Sigma}}^{-1}\mathbf{Q}_1\mathbf{Q}_2\ldots\mathbf{Q}_{L-1}. \tag{44}$$

Note that $\mathbf{Q}_l$ and $\mathbf{P}_l$, $l = 1, 2, \ldots, L$ are Givens rotation matrices, and hence, calculating (43) and (44) needs $O(M_t(K+L))$ and $O(M_r(K+L))$ flops, respectively.

We summarize the UCD-VBLAST scheme as follows:[2]

step	operation	flops
1	Compute SVD $\mathbf{H} = \mathbf{U}\mathbf{\Lambda}\mathbf{V}^*$	$O(M_tM_rK)$
2	Calculate $\mathbf{\Phi}^{1/2}$ using (6)	$O(K^2)$
3	$\mathbf{\Sigma} = \mathbf{\Lambda}\mathbf{\Phi}^{1/2}$	$O(K)$
4	Obtain $\tilde{\mathbf{\Sigma}}$ using (40)	$O(K)$
5	Apply GMD to $\tilde{\mathbf{\Sigma}}$ to obtain (41)	$O(L^2)$
6	Generate $\mathbf{F}$ using (43)	$O\left(M_t(K+L)\right)$
7	Compute $\mathbf{Q}_{G_a}^u$ using (44)	$O\left(M_r(K+L)\right)$
8	Calculate $\{\mathbf{w}_i\}_{i=1}^L$ using (35)	$O(M_rL)$

Obviously, our UCD-VBLAST scheme has comparable computational complexity to the SVD based linear transceiver designs. An observation relevant to practical implementations is as follows. Note that the receiver does not have to calculate Step 6 since CSIT is available, and the transmitter can run Steps 1 to 6. However, if the receiver calculates $\mathbf{F}$, which only takes a small number of flops, and feeds it back to the transmitter, then the transmitter is relieved from calculating the SVDs. Hence, in FDD systems, it is preferable to feed back $\mathbf{F}$, rather than $\mathbf{H}$, to the transmitter. In TDD systems, there are still advantages for feeding back $\mathbf{F}$ since this reduces by approximately half the overall computational complexity.

We conclude the discussions of the UCD-VBLAST scheme by deriving the SINR of each subchannel. Note that the diagonal elements of $\mathbf{R}_J$ is

$$r_{J,ii} = \left(\prod_{l=1}^L \tilde{\sigma}_l\right)^{\frac{1}{L}}, \quad i = 1, 2, \ldots, L \tag{45}$$

which is the geometric mean of the diagonal elements of $\tilde{\mathbf{\Sigma}}$. It follows from (40) that

$$r_{J,ii}^2 = \left(\alpha^{L-K}\prod_{l=1}^K\left(\sigma_l^2+\alpha\right)\right)^{\frac{1}{L}} = \alpha\left(\prod_{l=1}^K\left(\alpha^{-1}\sigma_l^2+1\right)\right)^{\frac{1}{L}}. \tag{46}$$

According to Lemma III.3

$$\rho_i := \bar{\rho} \triangleq \left(\prod_{l=1}^K\left(\alpha^{-1}\sigma_l^2+1\right)\right)^{\frac{1}{L}} - 1, \quad i=1,2,\ldots,L. \tag{47}$$

Hence

$$\sum_{i=1}^L \log_2(1+\rho_i) = \sum_{i=1}^K \log_2\left(1+\alpha^{-1}\sigma_i^2\right) = \sum_{i=1}^K \log_2\left(1+\alpha^{-1}\lambda_{H,i}^2\phi_i\right) \tag{48}$$

which is exactly the C_{IT} in (7). Hence, UCD-VBLAST is strictly capacity lossless.

[2]Steps 5–7 can be processed simultaneously as in the GMD algorithm.

B. UCD-DP

As a dual form of UCD-VBLAST, the UCD scheme can be implemented by using DP precoding, which we refer to as UCD-DP. For UCD-DP, a direct construction of the linear precoder $\mathbf{F}$, as done in Section IV-A, is not obvious. Instead, we exploit the uplink-downlink duality revealed in [17] to obtain UCD-DP.

We convert the UCD-DP problem into the UCD-VBLAST problem in the reverse channel, where the roles of the transmitter and receiver are exchanged:

$$\mathbf{y} = \mathbf{H}^*\mathbf{x} + \mathbf{z}. \tag{49}$$

The UCD-VBLAST scheme can be applied to the channel of (49), which yields the precoder $\mathbf{F}_{\text{rev}}$ and the equalizer $\{\mathbf{w}_i\}_{i=1}^L$, as in (43) and (35), respectively. Normalize $\{\mathbf{w}_i\}_{i=1}^L$ to be of unit Euclidean norm, which we denote as $\{\bar{\mathbf{w}}_i\}_{i=1}^L$. Let $\mathbf{W} = [\bar{\mathbf{w}}_1, \ldots, \bar{\mathbf{w}}_L]$. According to the uplink-downlink duality, the precoder of UCD-DP should be $\mathbf{F} = \mathbf{W}\mathbf{D}_q$, where $\mathbf{D}_q$ is diagonal with the diagonal elements $\{\sqrt{q_l}\}_{l=1}^L$, which will be determined based on (54) below. We use $\mathbf{F}_{\text{rev}}$, which is the linear precoder in the reverse channel, as the linear equalizer. Then, the equivalent MIMO channel is

$$\mathbf{y} = \mathbf{F}_{\text{rev}}^*\mathbf{H}\mathbf{W}\mathbf{D}_q\mathbf{x} + \mathbf{F}_{\text{rev}}^*\mathbf{z} \tag{50}$$

where the ith scalar subchannel of the MIMO channel is

$$y_i = \mathbf{f}_i^*\mathbf{H}\bar{\mathbf{w}}_i\sqrt{q_i}x_i + \sum_{j=i+1}^{L}\mathbf{f}_i^*\mathbf{H}\bar{\mathbf{w}}_j\sqrt{q_j}x_j + \sum_{j=1}^{i-1}\mathbf{f}_i^*\mathbf{H}\bar{\mathbf{w}}_j\sqrt{q_j}x_j + \mathbf{f}_i^*\mathbf{z}. \tag{51}$$

Applying the dirty paper precoder to x_i and treating $\sum_{j=1}^{i-1}\mathbf{f}_i^*\mathbf{H}\bar{\mathbf{w}}_j\sqrt{q_j}x_j$ as the interference known at the transmitter (note that here, we precode the first layer first, while for UCD-VBLAST, we detect the Lth layer first), we obtain an equivalent subchannel

$$y_i = \mathbf{f}_i^*\mathbf{H}\bar{\mathbf{w}}_i\sqrt{q_i}x_i + \sum_{j=i+1}^{L}\mathbf{f}_i^*\mathbf{H}\bar{\mathbf{w}}_j\sqrt{q_j}x_j + \mathbf{f}_i^*\mathbf{z} \tag{52}$$

with SINR

$$\rho_i = \frac{q_i\,|\mathbf{f}_i^*\mathbf{H}\bar{\mathbf{w}}_i|^2}{\alpha\|\mathbf{f}_i\|^2 + \sum_{j=i+1}^{L} q_j\,|\mathbf{f}_i^*\mathbf{H}\bar{\mathbf{w}}_j|^2}, \quad \text{for } i = 1, 2, \ldots, L. \tag{53}$$

The next step is to calculate $\{q_i\}_{i=1}^L$ such that $\rho_i = \bar{\rho}$, $1 \le i \le L$, where $\bar{\rho}$ is as defined in (47). Let $a_{ij} = |\mathbf{f}_i^*\mathbf{H}\bar{\mathbf{w}}_j|^2$. Then, (53) can be represented in the matrix form

$$\begin{bmatrix} a_{11} & -\bar{\rho}a_{12} & \cdots & -\bar{\rho}a_{1L} \\ 0 & a_{22} & \cdots & -\bar{\rho}a_{2L} \\ \vdots & \ddots & \ddots & \vdots \\ 0 & \cdots & 0 & a_{LL} \end{bmatrix} \begin{bmatrix} q_1 \\ q_2 \\ \vdots \\ q_L \end{bmatrix} = \bar{\rho}\alpha \begin{bmatrix} \|\mathbf{f}_1\|^2 \\ \|\mathbf{f}_2\|^2 \\ \vdots \\ \|\mathbf{f}_L\|^2 \end{bmatrix}. \tag{54}$$

It is easy to see that $q_i > 0$, $0 \le i \le L$. It is proven in [17] that $\sum_{i=1}^L q_i = \text{Tr}(\mathbf{F}\mathbf{F}^*) = \text{Tr}(\mathbf{F}_{\text{rev}}\mathbf{F}_{\text{rev}}^*)$. That is, the UCD-DP needs exactly the same power as the UCD-VBLAST to obtain L identical subchannels with SINR $\bar{\rho}$.

The UCD-DP using the Tomlinson–Harashima precoder leads to an input power increase of $M/(M-1)$ for M-QAM symbols. Nevertheless, for a system with high dimensionality and/or using large constellation, UCD-DP is a better choice than UCD-VBLAST since it is free of propagation errors.

C. Diversity Gain Analysis

Consider a channel given in (1). Assume, without loss of generality, that the rank of $\mathbf{H}$ is $K = \min(M_t, M_r)$, and let the number of identical subchannels be $L = K$ (GMD only allows $L \le K$). The output SINRs of the subchannels obtained via GMD and UCD are [cf. (15)]

$$\rho_{\text{GMD}} = \rho\bar{\lambda}_H^2 = \rho\left(\prod_{i=1}^{K}\lambda_{H,i}^2\right)^{\frac{1}{K}} \tag{55}$$

where ρ is the input SNR defined in (2), and [cf. (47)]

$$\rho_{\text{UCD}} = \left(\prod_{l=1}^{K}\left(\alpha^{-1}\sigma_l^2 + 1\right)\right)^{\frac{1}{K}} - 1 \tag{56}$$

where σ_l is the lth diagonal element of the $\mathbf{\Sigma}$ defined in (28) and is a function of ρ. One can verify that

$$\lim_{\rho\to\infty}\rho_{\text{UCD}}/\rho_{\text{GMD}} = 1 \tag{57}$$

i.e., the coding gain of the UCD scheme over the GMD scheme is asymptotically negligible for high SNR. It is a direct consequence of the fact that GMD is asymptotically for high SNR capacity lossless [5].

Another important performance metric is diversity gain, which is defined as follows [18].

Definition IV.2: Let $P_e(\rho)$ denote the average error probability of a scheme at SNR ρ. The diversity gain of the scheme is

$$d = -\lim_{\rho\to\infty}\frac{\log P_e(\rho)}{\log\rho}. \tag{58}$$

The diversity gain measures how fast the error probability decays with SNR. We note that diversity gain is usually discussed without assuming the availability of CSIT. The reason is that diversity gain is a concept associated with channel outage, i.e., the case where the channel is too poor to support a target data rate. Using CSIT, one can adjust the transmission rate to avoid channel outage. However, if the rate is fixed, which is desirable in practice, we can also use diversity gain as a performance measure of the transceiver designs. Based on this observation, we analyze the diversity gains of the UCD and GMD schemes. The result is summarized in the following proposition.

Proposition IV.3: Consider the i.i.d. Rayleigh flat fading MIMO channel defined in (1). Let $M = \max(M_t, M_r)$ and $m = \min(M_t, M_r)$. The diversity gains of the GMD and the UCD schemes are

$$d_{\text{GMD}}(M,m) = (M-m+1)m, \quad \text{and} \quad d_{\text{UCD}}(M,m) = Mm \tag{59}$$

respectively.

We have applied the *typical error event* analysis (see [18] and [19]) to obtain (59). The details are relegated to Appendix C. We see that although UCD has a negligible coding gain compared with the GMD scheme at high SNR, it has an additional $m^2 - m$ diversity gains over GMD. An interesting point to make is that

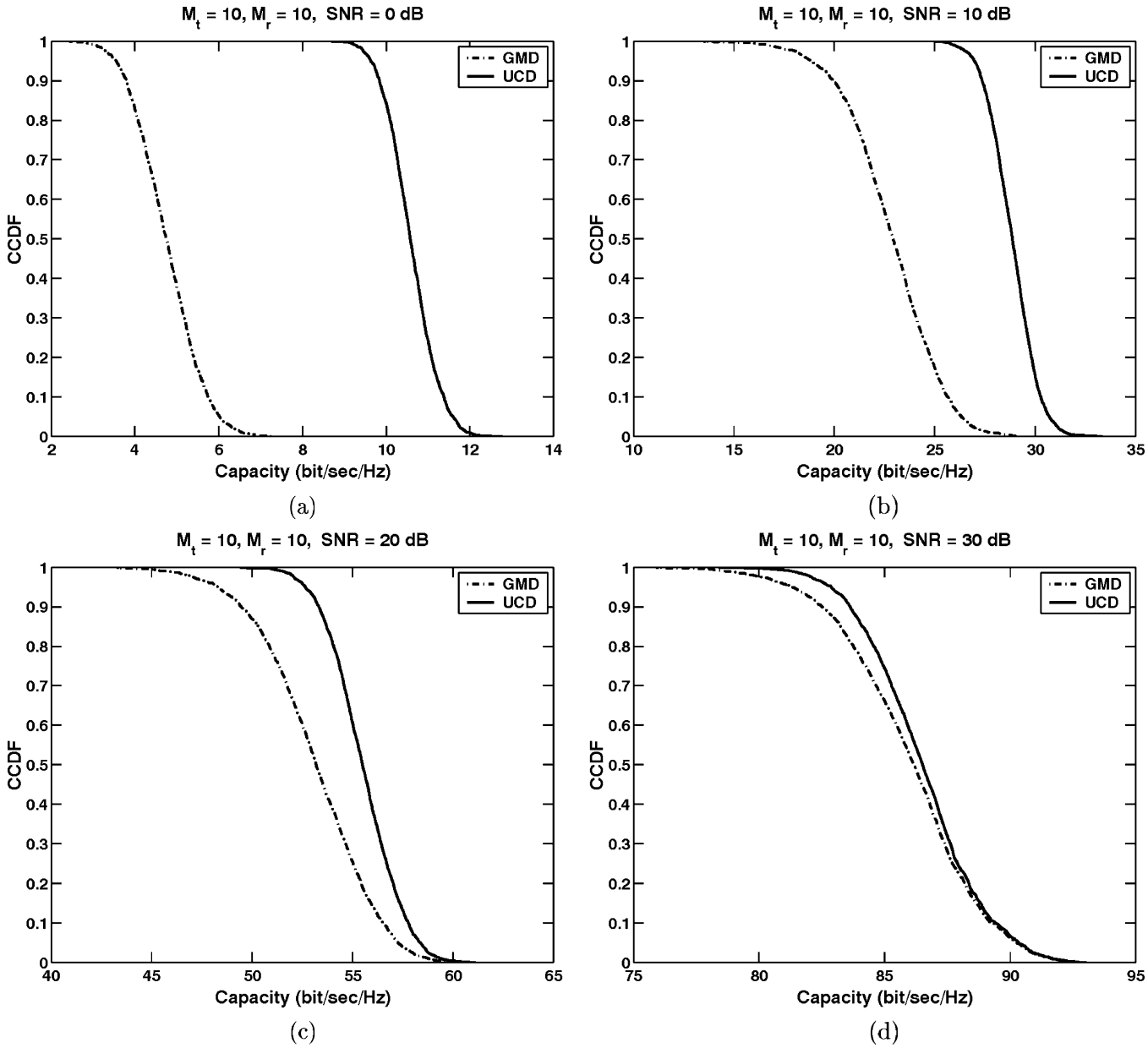

Fig. 1. Complementary cumulative distribution function of the capacity of an i.i.d. Rayleigh flat fading channel with $M_t = 10$ and $M_r = 10$. Results based on 2000 Monte Carlo trials. SNR is (a) 10 dB, (b) 10 dB, (c) 20 dB, and (d) 30 dB.

water filling does *not* help improve diversity gains. Hence, at high SNR, water filling is useless in both capacity and diversity aspects.

Given the fact that the GMD scheme is asymptotically capacity lossless for high SNR, it is rather surprising to see the large diversity loss of GMD compared with UCD. We give an intuitive explanation as follows. Note that diversity gain is determined by the typical error events that the MIMO channel is in deep fade. Namely, the diversity gain of a scheme depends on its ability to deal with bad channels. A deeply faded channel with high input SNR is equivalent to a "normal" channel with low SNR; in this scenario, the GMD scheme is far less efficient than UCD, as shown in the numerical examples. Consequently, the GMD has less diversity gain than UCD.

D. Further Remarks

Besides the larger coding gain at low SNR and an improved diversity gain at high SNR, the UCD scheme enjoys more flexibility than the GMD scheme. For a rank K MIMO channel, the GMD scheme can support no more than K independent data streams. However, the UCD scheme can decompose a rank K MIMO channel into $L \geq K$ *identical* subchannels, and L is *not* even limited by the dimensionality of the channel matrix. This property of the UCD scheme enables one to achieve high data rate transmission using small constellations as demonstrated in the numerical examples.

The UCD scheme also suggests new ways of channel decomposition that are much more flexible than the conventional SVD

based ones. Indeed, one may chose the permutation matrices and Givens rotations to achieve a wide variety of channel decompositions with some prescribed SINRs, as suggested by the generalized triangular decomposition (GTD) [8], [20].

Finally, we link UCD with DBLAST [2], which has been shown to be able to achieve the optimal tradeoff between the channel diversity and multiplexing [18]. We observe that each diagonal layer of DBLAST can be viewed as the interleaving of the vertical layers of VBLAST in the space-time domain, and each diagonal layer can be regarded as a virtual subchannel with the same capacity. However, DBLAST requires short and powerful error-correcting coding to make the *virtual* subchannel work as a "real" one. This is a major difficulty for the implementation of DBLAST. In addition, DBLAST suffers from boundary wastage. In contrast, our UCD scheme, by exploiting CSIT, applies interleaving (via the Givens rotations and permutations) in the space domain only. This makes the UCD scheme free from the boundary wastage. Moreover, the UCD scheme is decoupled from coding procedures. Indeed, UCD can be concatenated with any error-correcting code. Furthermore, UCD makes it easier to design the coding scheme since UCD decomposes a MIMO channel into multiple subchannels with *identical* capacities. Thus, in a slowly time-varying channel, UCD is much easier to implement than DBLAST, despite their duality. This clearly manifests the values of CSIT.

V. Numerical Examples

We present next several numerical examples to demonstrate the effectiveness of the UCD scheme.

In the first example, we assume Rayleigh independent flat fading channels with $M_t = 10$ and $M_r = 10$. We compare the channel capacity using the UCD and GMD schemes. The complementary cumulative distribution functions (CCDF) of the capacity drawn out of 2000 Monte Carlo realizations of $\mathbf{H}$ are shown in Fig. 1. We see that the UCD scheme outperforms the GMD scheme significantly at low SNR, although the difference becomes smaller at higher SNR.

Fig. 2 shows the CCDFs of the channel capacities of a 5×5 independent Rayleigh flat fading channel with SNR equal to 25 dB. The five thin dashed curves denote the channel capacities of the five subchannels obtained via SVD plus water filling. Note that the leftmost thin dashed curve crosses the vertical axis at a value less than one, which means that the worst subchannel (corresponding to the smallest singular value of the channel matrix) is sometimes discarded by water filling. The thick solid line is the CCDF of the capacity of the $L = 5$ subchannels obtained via UCD. All these subchannels have the same capacity. As discussed in Section IV-A, a rank K MIMO channel can be decomposed into $L \geq K$ subchannels. The thin solid line represents the case where a MIMO channel is decomposed into seven identical subchannels using the UCD scheme. Fig. 2 demonstrates the advantages of our UCD scheme over the conventional "SVD plus bit allocation" scheme (see, e.g., [4]). The channel capacities of the five subchannels obtained via SVD plus water filling range from 0 to about 11 bit/s/Hz, which suggests that the binary phase shift keying (BPSK) or quadrature phase shift keying (QPSK) modulation should be used to match

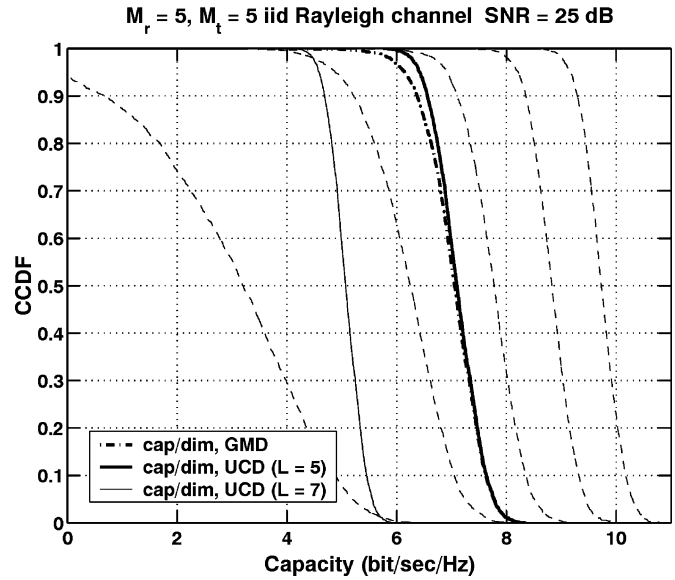

Fig. 2. Complementary cumulative distribution functions of the capacities of five subchannels of an i.i.d. Rayleigh flat fading channel with $M_t = 5$ and $M_r = 5$. Results based on 2000 Monte Carlo trials.

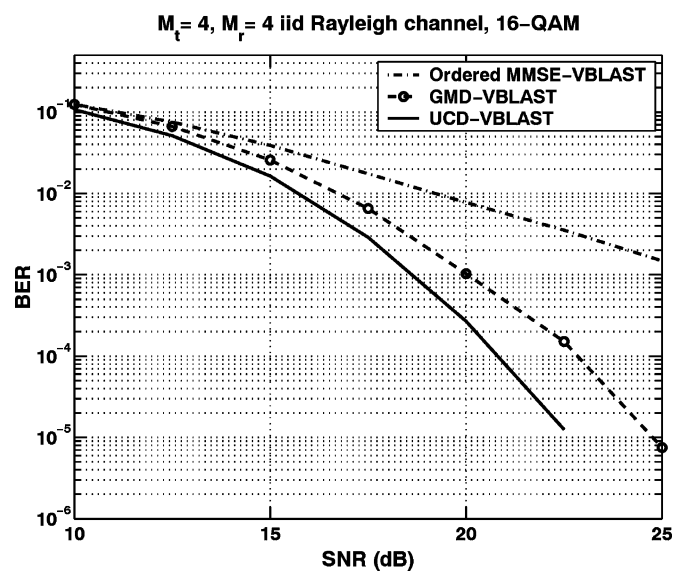

Fig. 3. Uncoded BER performance when using 16-QAM. Results based on 1000 Monte Carlo trials of an i.i.d. Rayleigh flat fading channel with $M_t = 4$ and $M_r = 4$.

the capacity of the worst subchannel and something like 1024 or 2048 quadrature amplitude modulation (QAM) to the best subchannel. This bit allocation significantly increases the modulation/demodulation complexity. Moreover, using a constellation with size greater than 256 is impractical for the current RF circuit design technology. Using GMD or UCD, we can decompose a rank 5 MIMO channel into five subchannels, and hence, the same constellation with a reasonable size, say 128-QAM, can be used to reap most of the channel capacity. The UCD scheme can do even better. In this example, after decomposing a MIMO channel into seven subchannels via UCD, we can apply a small to moderate constellation, say 16-QAM or 64-QAM, to achieve the channel capacity.

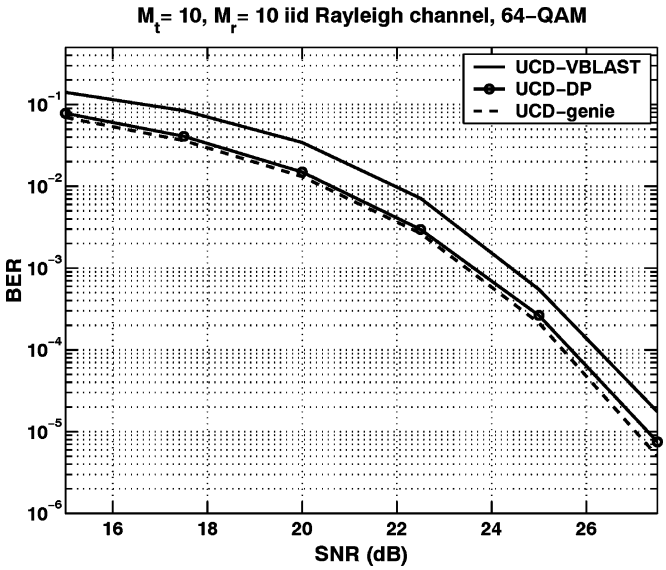

Fig. 4. BER performances of the UCD-DP, UCD-VBLAST schemes and the imaginary UCD-genie scheme. Results based on 1000 Monte Carlo trials of an i.i.d. Rayleigh flat fading channel with $M_t = 10$ and $M_r = 10$.

In the third example, we assume Rayleigh independent flat fading channels with $M_t = 4$ and $M_r = 4$. We compare the BER performance of the GMD and UCD schemes along with the conventional MMSE-VBLAST with optimal detection ordering in Fig. 3. We see that both GMD and UCD outperform the conventional VBLAST detector significantly. Moreover, the BER versus SNR lines of the GMD and UCD schemes have much steeper decreasing slopes, which means much better diversity gains than the conventional VBLAST. The diversity gains of the GMD and UCD schemes are 4 and 16, respectively. While there is a noticeably larger diversity gain for UCD compared with GMD, as shown in Fig. 3, the difference is not as drastic as the theoretical prediction. It is because the input SNR is not high enough to validate the approximations made in the typical error event analyses (see Appendix C).

In the final example, we compare the BER performance of UCD-VBLAST and UCD-DP in the scenario of a 10×10 Rayleigh flat fading channel. To present a benchmark, we also include UCD-genie as the imaginary scenario, where at each layer, a genie would eliminate the influence of erroneous detections from the previous layers when using UCD-VBLAST. Fig. 4 shows that UCD-VBLAST may suffer from some small BER degradations caused by error propagation (about 0.5 dB for BER $= 10^{-4}$) compared with UCD-genie. The UCD-DP, on the contrary, is free of error propagation and, hence, has a BER performance very close to that of UCD-genie. The slight SNR loss of UCD-DP is mainly due to the inherent power-amplification effect of the Tomlinson–Harashima precoder.

VI. Conclusions

Based on the GMD matrix decomposition algorithm and the closed-form representation of the MMSEVBLAST detector, we have introduced the UCD scheme for MIMO communications that can decompose a MIMO channel into multiple subchannels with *identical* capacities in a capacity lossless manner. We have proposed two versions of the UCD scheme, i.e., UCD-VBLAST and UCD-DP. The UCD scheme can provide much convenience for the subsequent modulation/demodulation and coding/decoding procedures due to obviating the need for bit allocation. We have also shown that UCD can achieve the maximal diversity gain. The simulations show that the UCD scheme has excellent performance even without the use of error-correcting codes. The UCD scheme suggests a new way of channel decomposition that enjoys much more flexibility than the conventional SVD-based ones.

Appendix A
Geometric Mean Decomposition

We now give an algorithm for evaluating the GMD that starts with the SVD $\mathbf{H} = \mathbf{U}\mathbf{\Lambda}\mathbf{V}^*$. The algorithm generates a sequence of upper triangular matrices $\mathbf{R}^{(\tilde{K})}$, $1 \le \tilde{K} < K$, with $\mathbf{R}^{(1)} = \mathbf{\Lambda}$. Each matrix $\mathbf{R}^{(\tilde{K})}$ has the following properties.

a) $r_{ij}^{(\tilde{K})} = 0$ when $i > j$ or $j > \max\{\tilde{K}, i\}$.

b) $r_{ii}^{(\tilde{K})} = \bar{\lambda}_H$ for all $i < \tilde{K}$, and the geometric mean of $r_{ii}^{(\tilde{K})}$, $\tilde{K} \le i \le K$, is $\bar{\lambda}_H$.

We express $\mathbf{R}^{(k+1)} = \mathbf{Q}_k^T \mathbf{R}^{(k)} \mathbf{P}_k$ where $\mathbf{Q}_k$ and $\mathbf{P}_k$ are orthogonal for each k.

These orthogonal matrices are constructed using a symmetric permutation and a pair of Givens rotations. Suppose that $\mathbf{R}^{(k)}$ satisfies a) and b). If $r_{kk}^{(k)} \ge \bar{\lambda}_H$, then let $\mathbf{\Pi}$ be a permutation matrix with the property that $\mathbf{\Pi}\mathbf{R}^{(k)}\mathbf{\Pi}$ exchanges the $(k+1)$st diagonal element of $\mathbf{R}^{(k)}$ with any element r_{pp}, $p > k$, for which $r_{pp} \le \bar{\lambda}_H$. If $r_{kk}^{(k)} < \bar{\lambda}_H$, then let $\mathbf{\Pi}$ be chosen to exchange the $(k+1)$st diagonal element with any element r_{pp}, $p > k$, for which $r_{pp} \ge \bar{\lambda}_H$. Let $\delta_1 = r_{kk}^{(k)}$ and $\delta_2 = r_{pp}^{(k)}$ denote the new diagonal elements at locations k and $k+1$ associated with the permuted matrix $\mathbf{\Pi}\mathbf{R}^{(k)}\mathbf{\Pi}$.

Next, we construct orthogonal matrices $\mathbf{G}_1$ and $\mathbf{G}_2$ by modifying the elements in the identity matrix that lie at the intersection of rows k and $k+1$ and columns k and $k+1$. We multiply the permuted matrix $\mathbf{\Pi}\mathbf{R}^{(k)}\mathbf{\Pi}$ on the left by $\mathbf{G}_2^T$ and on the right by $\mathbf{G}_1$. These multiplications will change the elements in the 2 by 2 submatrix at the intersection of rows k and $k+1$ with columns k and $k+1$. Our choice for the elements of $\mathbf{G}_1$ and $\mathbf{G}_2$ is shown below, where we focus on the relevant 2 by 2 submatrices of $\mathbf{G}_2^T\ \mathbf{\Pi}\mathbf{R}^{(k)}\mathbf{\Pi}$, and $\mathbf{G}_1$:

$$\underbrace{\bar{\lambda}_H^{-1}\begin{bmatrix} c\delta_1 & s\delta_2 \\ -s\delta_2 & c\delta_1 \end{bmatrix}}_{(\mathbf{G}_2^T)} \underbrace{\begin{bmatrix} \delta_1 & 0 \\ 0 & \delta_2 \end{bmatrix}}_{(\mathbf{\Pi}\mathbf{R}^{(k)}\mathbf{\Pi})} \underbrace{\begin{bmatrix} c & -s \\ s & c \end{bmatrix}}_{(\mathbf{G}_1)} = \underbrace{\begin{bmatrix} \bar{\lambda}_H & x \\ 0 & y \end{bmatrix}}_{(\mathbf{R}^{(k+1)})}. \tag{60}$$

If $\delta_1 = \delta_2 = \bar{\lambda}_H$, we take $c = 1$ and $s = 0$; if $\delta_1 \ne \delta_2$, we take

$$c = \sqrt{\frac{\tilde{\lambda}_H^2 - \delta_2^2}{\delta_1^2 - \delta_2^2}} \quad \text{and} \quad s = \sqrt{1 - c^2}. \tag{61}$$

Since $\bar{\lambda}_H$ lies between δ_1 and δ_2, s and c are non-negative real-valued scalars.

Fig. 5 depicts the transformation from $\mathbf{R}^{(k)}$ to $\mathbf{G}_2^T\mathbf{\Pi}\mathbf{R}^{(k)}\mathbf{\Pi}\mathbf{G}_1$. The dashed box is the 2 by 2 submatrix displayed in (60). Note that c and s, which are defined in (61), are real-valued scalars chosen so that

$$c^2 + s^2 = 1 \quad \text{and} \quad (c\delta_1)^2 + (s\delta_2)^2 = \bar{\lambda}_H^2.$$

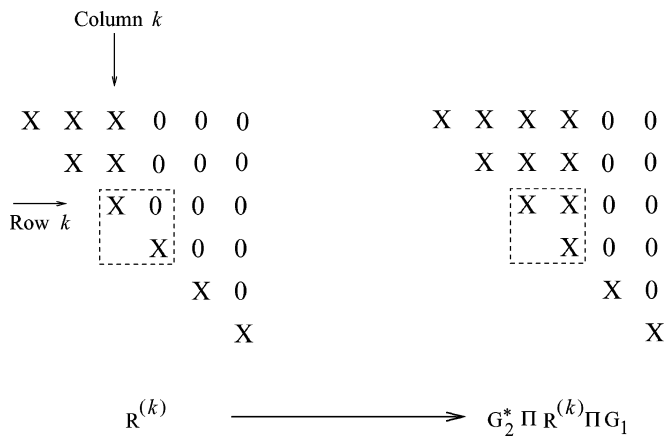

Fig. 5. Operation displayed in (60).

With these identities, the validity of (60) follows by direct computation. Defining $\mathbf{Q}_k = \mathbf{\Pi}\mathbf{G}_2$ and $\mathbf{P}_k = \mathbf{\Pi}\mathbf{G}_1$, we set

$$\mathbf{R}^{(k+1)} = \mathbf{Q}_k^T \mathbf{R}^k \mathbf{P}_k. \tag{62}$$

It follows from Fig. 5, (60), and the identity $|\mathbf{R}^{(k+1)}| = |\mathbf{R}^{(k)}|$, that a) and b) hold for $\tilde{K} = k+1$. Thus, there exists a real-valued upper triangular matrix $\mathbf{R}^{(K)}$ with $\bar{\lambda}_H$ on the diagonal and unitary matrices $\mathbf{Q}_i$ and $\mathbf{P}_i$, $i = 1, 2, \ldots, K-1$, such that

$$\mathbf{R}^{(K)} = \left(\mathbf{Q}_{K-1}^T \ldots \mathbf{Q}_2^T \mathbf{Q}_1^T\right) \mathbf{\Lambda}(\mathbf{P}_1 \mathbf{P}_2 \ldots \mathbf{P}_{K-1}).$$

Combining this identity with the SVD, we obtain $\mathbf{H} = \mathbf{Q}\mathbf{R}\mathbf{P}^*$, where

$$\mathbf{Q} = \mathbf{U}\left(\prod_{i=1}^{K-1} \mathbf{Q}_i\right), \quad \mathbf{R} = \mathbf{R}^{(K)}, \quad \text{and } \mathbf{V}\left(\prod_{i=1}^{K-1} \mathbf{P}_i\right).$$

A Matlab implementation of this algorithm for the GMD is posted at the following web site: http://www.sal.ufl.edu/yjiang/papers/gmd.m. Given the SVD, this algorithm for the GMD requires $O((M_r + M_t)K)$ flops. For comparison, reduction of $\mathbf{H}$ to bidiagonal form by the Golub–Kahan bidiagonalization scheme [21], which is often the first step in the computation of the SVD, requires $O(M_r M_t K)$ flops.

Appendix B
Proof of Lemma III.3

Rewrite (21)

$$\mathbf{H}_a = \mathbf{Q}_{H_a}\mathbf{R}_{H_a} \triangleq \begin{bmatrix} \mathbf{Q}_{H_a}^u \\ \mathbf{Q}_{H_a}^l \end{bmatrix} \mathbf{R}_{H_a}. \tag{63}$$

Let $\mathbf{H}_{ai}(\mathbf{H}_i)$ denote the submatrix containing the first i columns of $\mathbf{H}_a(\mathbf{H})$ and $\mathbf{h}_{ai}(\mathbf{h}_i)$ the ith column. Then

$$\mathrm{H}_{a,i} = \begin{bmatrix} \mathbf{H}_i \\ \sqrt{\alpha}\mathbf{I}_i \\ \mathbf{0}_{(M_i - i)\times M_t} \end{bmatrix}, \quad \mathbf{h}_{a,i} = \begin{bmatrix} \mathbf{h}_i \\ \mathbf{0}_{(i-1)\times 1} \\ \sqrt{\alpha} \\ \mathbf{0}_{(M_t - i)\times 1} \end{bmatrix}. \tag{64}$$

For the QR decomposition $\mathbf{H}_a = \mathbf{Q}_{H_a}\mathbf{R}_{H_a}$, the geometric implication of $r_{H_a,ii}$ is the component of $\mathbf{h}_{ai}$ projected onto the subspace spanned by the ith column of $\mathbf{Q}_{H_a}$, i.e., $\mathbf{q}_{H_a,i}$. Note that $\mathbf{q}_{H_a,i}$ is orthogonal to the subspace spanned by $\{\mathbf{q}_{H_a,i}\}_{j=1}^{i-1}$, or equivalently, the column space of $\mathbf{H}_{a,i-1}$. Hence

$$r_{H_a,ii}^2 = \mathbf{h}_{a,i}^* \mathcal{P}_{\mathbf{H}_{a,i-1}}^{\perp} \mathbf{h}_{a,i} \tag{65}$$

where $\mathcal{P}_{\mathbf{A}}^{\perp}$ stands for the orthogonal projection onto th null space of $\mathbf{A}^T$. Therefore

$$r_{H_a,i}^2 = \mathbf{h}_{a,i}^* \left[\mathbf{I} - \mathbf{H}_{a,i,-1}\left(\mathbf{H}_{a,i-1}^*\mathbf{H}_{a,i-1}\right)^{-1}\mathbf{H}_{a,i-1}^*\right]\mathbf{h}_{a,i}. \tag{66}$$

Inserting (64) into (66) yields

$$\begin{aligned} r_{H_a,ii}^2 &= \alpha + \mathbf{h}_i^* \left[\mathbf{I} - \mathbf{H}_{i,-1}\left(\mathbf{H}_{i-1}^*\mathbf{H}_{i-1} + \alpha\mathbf{I}\right)^{-1}\mathbf{H}_{i-1}^*\right]\mathbf{h}_i \\ &= \alpha + \alpha\mathbf{h}_i^*\left(\mathbf{H}_{i-1}\mathbf{H}_{i-1}^* + \alpha\mathbf{I}\right)^{-1}\mathbf{h}_i. \end{aligned} \tag{67}$$

From (24), we see that

$$\rho_i = \mathbf{h}_i^*\left(\mathbf{H}_{i-1}\mathbf{H}_{i-1}^* + \alpha\mathbf{I}\right)^{-1}\mathbf{h}_i. \tag{68}$$

Hence, $r_{H_a,ii}^2 = \alpha(1 + \rho_1)$. The lemma is proven.

Appendix C
Proof of Proposition IV.3

Without loss of generality, we assume $\mathbf{H} \in \mathbb{C}^{M\times m}$, where each entry is of circularly symmetric Gaussian distribution with zero-mean and unit variance. Consider BPSK modulation. The average error probability of the GMD scheme is

$$\begin{aligned} P_e^{\mathrm{GMD}} &= E\left[Q(\sqrt{2\rho_{\mathrm{GMD}}})\right] \\ &= E\left[Q\left(\sqrt{2\rho\bar{\lambda}_H^2}\right)\right] \\ &= E\left[Q\left(\sqrt{2\rho\left(\prod_{i=1}^{m}\lambda_{H,i}^2\right)^{\frac{1}{m}}}\right)\right] \end{aligned} \tag{69}$$

where the Q-function is defined as

$$Q(x) = \int_x^{+\infty} \frac{1}{2\pi} e^{-\frac{x^2}{2}} dx.$$

The diversity gain of the CMD scheme is

$$d_{\mathrm{GMD}}(M, m) = -\lim_{\rho\to\infty} \frac{\log P_e^{\mathrm{GMD}}}{\log\rho}. \tag{70}$$

For any QAM constellation, the average error probability is similar to (69), except for some constants before or inside the Q-function. Since we focus on the high SNR region, all these constants will not affect the diversity gain defined in (70).

At high SNR, the *typical error event* is

$$\mathcal{E} = \left\{\bar{\lambda}_H : \bar{\lambda}_H^2 < \rho^{-1}\right\}. \tag{71}$$

It can be shown that instead of calculating (70), which involves complicated integrations, we can compute the following [19, Ch. 3]:

$$d_{\mathrm{GMD}}(M, m) = -\lim_{\rho\to\infty} \frac{\log P(\mathcal{E})}{\log\rho}. \tag{72}$$

Note that

$$\bar{\lambda}_H^{2m} = \prod_{i=1}^{m} \lambda_{H,i}^2 = |\mathbf{H}^*\mathbf{H}|. \tag{73}$$

According to [22, Th. 7.5.3] (with straightforward extensions from real-valued domain to the complex-valued domain)

$$\bar{\lambda}_H^{2m} = |\mathbf{H}^*\mathbf{H}| = \prod_{i=1}^{m} g_{M-m+i}^2 \tag{74}$$

where g_i^2's are independent Chi-squared random variables with probability density

$$f_{g_i^2}(x) = \frac{1}{(i-1)!} x^{i-1} e^{-x}, \quad x \geq 0. \tag{75}$$

Now the typical error event can be written as

$$\begin{aligned}\mathcal{E} &= \left\{ \{g_{M-m+i}^2\}_{i=1}^m : \prod_{i=1}^{m} g_{M-m+1}^2 < \rho^{-m} \right\} \\ &= \bigcup_{\{a_i\}_{i=1}^m \in \mathcal{E}_\alpha} \Big\{ \{g_{M-m+1}^2\}_{i=1}^m : \\ &\qquad g_{M-m+i}^2 < \rho^{-\alpha_i},\ i=1,\ldots,m \Big\}\end{aligned} \tag{76}$$

where $\mathcal{E}_\alpha = \{\{\alpha_i\}_{i=1}^m : \sum_{i=1}^m \alpha_i > m\}$. Hence

$$P(\mathcal{E}) = \int_{\mathcal{E}_\alpha} \prod_{i=1}^{m} P\left(g_{M-m+1}^2 < \rho^{-\alpha_i}\right) d\alpha_1 \ldots d\alpha_m. \tag{77}$$

From (75), we know that as $\epsilon \to 0$

$$\begin{aligned}P\left(g_i^2 < \epsilon\right) &= \int_0^\epsilon \frac{1}{(i-1)!} x^{i-1} e^{-x} dx \\ &\approx \int_0^\epsilon \frac{1}{(i-1)!} x^{i-1} dx \\ &= \frac{1}{i!}\epsilon^i.\end{aligned} \tag{78}$$

Using (72), (77), and (78), we calculate the diversity gain as

$$\begin{aligned}&d_{\mathrm{GMD}}(M,m) \\ &= -\lim_{\rho\to\infty} \frac{\log \int_{\mathcal{E}_\alpha^+} \prod_{i=1}^m \frac{\rho^{-(M-m+i)\alpha_i}}{(M-m+i)!} d\alpha_1 \ldots d\alpha_m.}{\log \rho} \\ &= -\lim_{\rho\to\infty} \frac{\log \int_{\mathcal{E}_\alpha^+} \rho^{-\sum_{i=1}^m (M-m+i)\alpha_i} d\alpha_1 \ldots d\alpha_m.}{\log \rho} \qquad (79) \\ &= \inf_{\mathcal{E}_\alpha^+} \sum_{i=1}^{m} (M-m+i)\alpha_i \qquad (80)\end{aligned}$$

where $\mathcal{E}_\alpha^+ = \varepsilon_\alpha \bigcap \{\alpha_i > 0, i = 1.\ldots,m\}$. To obtain (80) from (79), we have used the property that the integral in the numerator of (79) is dominated by the term with the SNR exponent closest to zero, as $\rho \to \infty$ (see [18] for details). Here, the integration is constrained over $\mathcal{E}_\alpha^+$ because the integration over $\mathcal{E}_\alpha$ is dominated by the one over $\mathcal{E}_\alpha^+$. The reason is as follows. Suppose only $\alpha_{n_1}, \ldots, \alpha_{n_j} > 0, j < m$, and the other αs $\alpha_{k_1}, \ldots, \alpha_{k_{m-j}}$ are negative. Then

$$\begin{aligned}\prod_{i=1}^{m} P\left(g_{M-m+i}^2 < \rho^{-\alpha_i}\right) &\approx \prod_{i=1}^{j} P\left(g_{M-m+n_i}^2 < \rho^{-\alpha_{n_i}}\right) \\ &\approx \rho^{-\sum_{i=1}^{j}(M-m+n_i)\alpha_{n_i}}.\end{aligned}$$

Let $\tilde{\mathcal{E}}_\alpha^+$ denote $\{\{\alpha_{n_i}\}_{i=1}^j > 0 : \sum_{i=1}^j \alpha_{n_i} > m - \sum_{i=1}^{m-j} \alpha_{k_i}\}$. Clearly

$$\inf_{\tilde{\mathcal{E}}_\alpha^+} \sum_{i=1}^{j} (M-m+n_i)\alpha_{n_i} > \inf_{\tilde{\mathcal{E}}_\alpha^+} \sum_{i=1}^{m} (M-m+i)\alpha_i$$

which implies that the integration over $\mathcal{E}_\alpha$ is dominated by that over $\mathcal{E}_\alpha^+$. Solving the optimization problem of (80) yields

$$d_{\mathrm{GMD}}(M,m) = (M-m+1)m. \tag{81}$$

Now, we consider UCD. We observe that the power allocation applied to each eigen subchannel is no greater than ρ. Hence, the overall channel throughput of UCD is

$$\sum_{i=1}^{m} \log\left(1 + \frac{\rho}{m}\lambda_{H,i}^2\right) \leq R_{\mathrm{UCD}} \leq \sum_{i=1}^{m} \log\left(1 + \rho\lambda_{H,i}^2\right) \tag{82}$$

where the left term denotes the channel throughput associated with uniform power allocation. Applying UCD, we obtain m subchannels with the same SNR:

$$\sqrt[m]{\prod_{i=1}^{m}\left(1 + \frac{\rho}{m}\lambda_{H,i}^2\right)} - 1 \leq \rho_{\mathrm{UCD}} \leq \sqrt[m]{\prod_{i=1}^{m}\left(1 + \rho\lambda_{H,i}^2\right)} - 1. \tag{83}$$

The typical error event is

$$\mathcal{E} = \{\{\lambda_{H,i}\}_{i=1}^m : \rho_{\mathrm{UCD}} < 1\}. \tag{84}$$

It follows from (83) that

$$\begin{aligned}P_1(\rho) &\triangleq P\left(\sqrt[m]{\prod_{i=1}^{m}\left(1+\frac{\rho}{m}\lambda_{H,i}^2\right)} - 1 < 1\right) \geq P(\mathcal{E}) \\ &\geq P\left(\sqrt[m]{\prod_{i=1}^{m}\left(1+\rho\lambda_{H,i}^2\right)} - 1 < 1\right) \triangleq P_2(\rho).\end{aligned} \tag{85}$$

It is easy to see that

$$\lim_{\rho\to\infty} \frac{\log P_1(\rho)}{\log \rho} = \lim_{\rho\to\infty} \frac{\log P_2(\rho)}{\log \rho}. \tag{86}$$

Hence

$$\lim_{\rho\to\infty} \frac{\log P(\mathcal{E})}{\log \rho} = \lim_{\rho\to\infty} \frac{\log P_1(\rho)}{\log \rho} \tag{87}$$

which implies that water filling does *not* help improve diversity gain.

It follows from the analyses of [18] that the UCD scheme achieves the optimal diversity-multiplexing tradeoff. In particular, when the transmission data rate is fixed, disregard the increase of input SNR, and the diversity gain is $d_{\mathrm{ucd}}(M,m) = Mm$.

ACKNOWLEDGMENT

The authors are grateful to the anonymous reviewers for their helpful suggestions for improving the submitted manuscript. The authors thank Dr. L. Yang for the inspiring discussions on diversity gain.

REFERENCES

[1] I. E. Telatar, Capacity of multiple antenna Gaussian channels, in AT&T Tech. Memo., Jun. 1995.

[2] G. J. Foschini Jr., "Layered space-time architecture for wireless communication in a fading environment when using multi-element antennas," *Bell Labs Tech. J.*, vol. 1, pp. 41–59, Autumn 1996.

[3] D. Palomar, J. Cioffi, and M. Lagunas, "Joint Tx-Rx beamforming design for multicarrier MIMO channels: a unified framework for convex optimization," *IEEE Trans. Signal Process.*, vol. 51, no. 9, pp. 2381–2401, Sep. 2003.

[4] G. G. Raleigh and J. M. Cioffi, "Spatial-temporal coding for wireless communication," *IEEE Trans. Commun.*, vol. 46, no. 3, pp. 357–366, Mar. 1998.

[5] Y. Jiang, J. Li, and W. Hager, "Joint transceiver design for MIMO communications using geometric mean decomposition," *IEEE Trans. Signal Process.*, vol. 53, no. 10, pt. 1, pp. 3791–3803, Oct. 2005.

[6] Y. Jiang, W. Hager, and J. Li, "The geometric mean decomposition," *Linear Algebra and Its Applications*, vol. 396, pp. 373–384, Feb. 2005.

[7] G. J. Foschini, G. D. Golden, R. A. Valenzuela, and P. W. Wolniansky, "Simplified processing for high spectral efficiency wireless communication employing multiple-element arrays," *Wireless Pers. Commun.*, vol. 6, pp. 311–335, March 1999.

[8] Y. Jiang and J. Li, "Adaptable channel decomposition for MIMO communications," in *Proc. IEEE Int. Conf. Acoust., Speech, Signal Process.*, 2005.

[9] I. E. Telatar, "Capacity of multi-antenna Gaussian channels," *Eur. Trans. Telecommun.*, vol. 10, no. 6, pp. 585–595, 1999.

[10] G. Caire and S. Shamai, "On the achievable throughput of a multiantenna Gaussian broadcast channel," *IEEE Trans. Inf. Theory*, vol. 49, no. 7, pp. 1691–1706, Jul. 2003.

[11] G. Ginis and J. M. Cioffi, "A multi-user precoding scheme achieving crosstalk cancellation with application to DSL systems," in *Proc. 34th Asilomar Conf. Signals, Syst., Comput.*, vol. 2, Asilomar, CA, 29 Oct.–1 Nov. 2000, pp. 1627–1631.

[12] M. Costa, "Writing on dirty paper," *IEEE Trans. Inf. Theory*, vol. IT–29, no. 3, pp. 439–441, May 1983.

[13] M. Tomlinson, "New automatic equaliser employing modulo arithmetic," *Electron. Lett.*, vol. 7, pp. 138–139, Mar. 1971.

[14] B. Hassibi, "A fast square-root implementation for BLAST," in *Proc. Thirty-Fourth Asilomar Conf. Signals, Syst., Comput.*, Nov. 2000, pp. 1255–1259.

[15] ——, (2000) An Efficient Square-Root Implementation for BLAST. [Online]http://cm.bell-labs.com/who/hochwald/papers/squareroot/

[16] M. Varanasi and T. Guess, "Optimum decision feedback multiuser equalization with successive decoding achieves the total capacity of the Gaussian multiple-access channel," in *Conf. Rec. Thirty-First Asilomar Conf. Signals, Syst., Comput.*, vol. 2, Nov. 2–5, 1997, pp. 1405–1409.

[17] P. Viswanath and D. Tse, "Sum capacity of the vector Gaussian broadcast channel and uplink-downlink duality," *IEEE Trans. Inf. Theory*, vol. 49, no. 8, pp. 1912–1921, Aug. 2003.

[18] L. Zheng and D. Tse, "Diversity and multiplexing: a fundamental tradeoff in multiple-antenna channels," *IEEE Trans. Inf. Theory*, vol. 49, no. 5, pp. 1073–1096, May 2003.

[19] D. Tse and P. Viswanath, *Fundamentals of Wireless Communications*. Cambridge, U.K.: Cambridge Univ. Press, May 2005.

[20] Y. Jiang, W. Hager, and J. Li, "The generalized triangular decomposition," *SIAM J. Matrix Anal. Appl.*, submitted for publication.

[21] G. H. Golub and C. F. Van Loan, *Matrix Computations*. Baltimore, MD: Johns Hopkins Univ. Press, 1983.

[22] T. W. Anderson, *An Introduction to Multivariate Statistical Analysis*, Second ed. New York: Wiley, 1984.

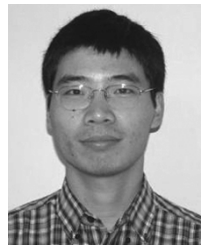

Yi Jiang (S'02) received the B.Sc. degree in electrical engineering and information science from the University of Science and Technology of China (USTC), Hefei, China, in 2001. He received the M.Sc. and Ph.D. degrees from the University of Florida, Gainesville, both in electrical engineering, in 2003 and 2005, respectively.

In the summer of 2005, he was a Research Consultant with Information Science Technologies, Inc. (ISTI), Fort Collins, CO. He is now a Postdoctoral Researcher with the University of Colorado, Boulder. His research interests are in the areas of signal processing, wireless communications, and information theory.

Jian Li (S'87–M'91–SM'97–F'05) received the M.Sc. and Ph.D. degrees in electrical engineering from The Ohio State University (OSU), Columbus, in 1987 and 1991, respectively.

From April 1991 to June 1991, she was an Adjunct Assistant Professor with the Department of Electrical Engineering, OSU. From July 1991 to June 1993, she was an Assistant Professor with the Department of Electrical Engineering, University of Kentucky, Lexington. Since August 1993, she has been with the Department of Electrical and Computer Engineering, University of Florida, Gainesville, where she is currently a Professor. Her current research interests include spectral estimation, statistical and array signal processing, sensor networks, machine learning, and their applications.

Dr. Li is a Fellow of the IEE. She is a member of Sigma Xi and Phi Kappa Phi. She received the 1994 National Science Foundation Young Investigator Award and the 1996 Office of Naval Research Young Investigator Award. She was an Executive Committee Member of the 2002 International Conference on Acoustics, Speech, and Signal Processing, Orlando, FL, May 2002. She has been an Associate Editor of the IEEE TRANSACTIONS ON SIGNAL PROCESSING since 1999 and an Associate Editor of the IEEE SIGNAL PROCESSING MAGAZINE since 2003. She is presently a member of both the IEEE Signal Processing Theory and Methods (SPTM) Technical Committee and the Sensor Array and Multichannel (SAM) Technical Committee.

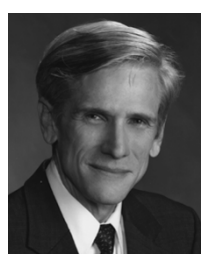

William W. Hager received the B.S. degree in mathematics from Harvey Mudd College, Claremont, CA, in 1970. He received a National Science Foundation Fellowship for graduate studies in mathematics at the Massachusetts Institute of Technology, Cambridge, from which he received the Masters and Ph.D. degrees in 1971 and 1974, respectively.

He has held positions at the University of South Florida, Tampa, from 1974 to 1976, where he was an Assistant Professor; Carnegie Mellon University, Pittsburgh, PA, from 1976 to 1980, where he was an Assistant Professor, Penn State University, University Park, from 1980 to 1986, as an Associate Professor and from 1986 to 1988 as a Professor; and the University of Florida, Gainesville, since 1988, as a Professor.

Dr.. Hager has been editor-in-chief of *Computational Optimization and Applications* and co-Director of the Center for Applied Optimization at the University of Florida since 1992. He was Program Director of the SIAM Activity Group on Control and System Theory from 1998 to 2001, and co-chair of the 2001 SIAM Conference on Control and Its Applications.